

PKU-TP-98-51

Diffractive charm jet production at hadron colliders in the two-gluon exchange model

Feng Yuan

Department of Physics, Peking University, Beijing 100871, People's Republic of China

Kuang-Ta Chao

China Center of Advanced Science and Technology (World Laboratory), Beijing 100080, People's Republic of China

and Department of Physics, Peking University, Beijing 100871, People's Republic of China

Abstract

We present a calculation of diffractive charm jet production at hadron colliders in perturbative QCD based on the two-gluon exchange model. Differing from the previous calculations, we abandon the use of the effective color-singlet virtual gluon simplification, and use the real gluon in the calculations for the partonic process. We find the final result is free of the linear singularities due to the small transverse momenta of the exchanged two gluons. In the leading logarithmic approximation (LLA) in QCD, this process is related to the off-diagonal gluon density in the proton. As a result, this process may provide a wide window for testing the two-gluon exchange model, and may be particularly useful in studying the small x physics. In comparison, the diffractive bottom jet production is also discussed, and is found to be important only for large transverse momentum of the jet.

PACS number(s): 12.40.Nn, 13.85.Ni, 14.40.Gx

Typeset using REVTeX

I. INTRODUCTION

In recent years, there has been a renaissance of interest in diffractive scattering. These diffractive processes are described by the Regge theory in terms of the Pomeron (\mathcal{P}) exchange [1]. The Pomeron carries quantum numbers of the vacuum, so it is a colorless entity in QCD language, which may lead to the “rapidity gap” events in experiments. However, the nature of the Pomeron and its interaction with hadrons remain a mystery. For a long time it had been understood that the dynamics of the “soft Pomeron” was deeply tied to confinement. However, it has been realized now that much can be learned about QCD from the wide variety of small- x and hard diffractive processes, which are now under study experimentally. Of all these processes, the diffractive heavy quark and quarkonium production have drawn specially attention, because their large masses provide a natural scale to guarantee the application of perturbative QCD [2–4]. In the framework of perturbative QCD the Pomeron is assumed to be represented by a pair of gluons in the color-singlet state. An important feature of this perturbative QCD model prediction is that the cross section for the diffractive processes is expressed in terms of the off-diagonal gluon distribution in the proton [5].

So far the previous studies are focused on the diffractive processes at ep collider (photoproduction and DIS processes), we should expect that the two-gluon exchange model can also be used to describe the diffractive processes at hadron colliders. Recently, we have extended the idea of perturbative QCD description of diffractive processes from ep colliders to hadron colliders [6], in which the hadronic diffractive J/ψ production is calculated in the two-gluon exchange model. In this paper, we will calculate the diffractive charm jet production at hadron colliders in this two-gluon exchange model. For a theoretical point of view the study of diffractive charm jet production has some advantages compared to J/ψ production, because it avoids the ambiguities associated with the color-octet production matrix elements [7,6] and retains the sensitivity to the off-diagonal gluon density in the proton.

However, there exist nonfactorization effects in the hard diffractive processes at hadron collisions [8–11]. These effects mainly focus on the following two sides. One is the so-called spectator effects [10]. The interaction with the spectator quarks can change the probability of the diffractive hadron emerging from collisions intact. This implies that the extra interaction with spectators makes it less likely for the diffractive hadron to survive [12]. Typically, for the diffractive processes at the Tevatron, this survival probability is shown to be about 0.1 [10,11]. The other one is the “coherent diffractive” processes, in which the whole Pomeron is involved in the hard process. These coherent diffractive processes have been proved to break the factorization assumption of [13].

As shown in Fig.1, the diffractive charm jet production process $p\bar{p} \rightarrow c\bar{c}p$ calculated in this paper belongs to these coherent diffractive processes. The whole Pomeron represented by the color-singlet two-gluon system emitted from one hadron interacts with another hadron to produce the charm jets. In the leading order perturbative QCD, the partonic process $gp \rightarrow c\bar{c}p$ is plotted in Fig.2. In the diffractive final states, there are only charm and anticharm jets balanced in the transverse momentum distribution. Experimentally, this would provide a strong signal for the coherent diffractive processes at hadron colliders.

The diffractive production of heavy quark jet at hadron colliders has also been studied in Ref. [14]. However, our calculation is quite different from theirs. In their calculation

of the partonic process $gp \rightarrow c\bar{c}p$, they used an effective color-singlet virtual gluon (as a color-singlet probe in their language) to replace the real gluon for simplification. In our calculations, we abandon this simplification, and use the real gluon in the calculations of the partonic process. This of course will cause more complicated calculations. However, after a lengthy calculation which will be shown in the following we find that our result is free of linear singularities, and then guarantees the gauge invariance of QCD.

Another important difference between [14] and our calculations is the definition of the coherent diffraction. Following Ref. [9], we call the process in which the whole Pomeron participants in the hard scattering process as the coherent diffractive process. Under this definition, all of the nine diagrams of Fig.2 contribute to the coherent diffractive production of heavy quark jet. However, in [14] they separate their diagrams into two parts: one part (the first four diagrams) contributes to the conventional IS model diffraction; and the other part contributes to the so-called coherent diffraction. However, in our calculations, the first four diagrams in Fig.2 alone do not contribute a gauge invariant part of the amplitude, and their sum will lead to a linear singularity which is not proper in QCD calculations. So, for a full calculation, the nine diagrams must be summed together to contribute to the coherent diffraction.

Another important issue of this process is about the gluon (off-diagonal) distribution in the proton at small x . As shown in Ref. [6], in hadron collisions (such as at the Tevatron), we can explore the gluon distribution at small x down to 10^{-6} by studying the hard diffractive J/ψ production. In the diffractive charm jet production, the involved gluon distribution function may take its value at the same order as that for J/ψ production. So, detecting the diffractive charm jet production at hadron colliders is also attractive for the study of the small x physics. Furthermore, experimentally the diffractive charm jet production is easily detected because the diffractive final states of c and \bar{c} pair may have large transverse momenta distribution.

The rest of the paper is organized as follows. In Sec.II, we give the cross section formula for the partonic process $gp \rightarrow c\bar{c}p$ in the leading logarithmic approximation (LLA) QCD. We use the Feynman rule method in the calculations. We also check our method to reproduce the formula for the diffractive charm jet production in the photoproduction processes previous calculated by others [4]. The numerical results are given in Sec.III for diffractive charm jet production at the Fermilab Tevatron. In Sec.IV, we give some discussions about the off-diagonal distribution effects on the process calculated here and the J/ψ production of [6]. The conclusion is given in Sec.V.

II. LLA FORMULA FOR THE PARTONIC PROCESS

As sketched in Fig.1, the cross section for the diffractive charm jet production at hadron colliders ($p\bar{p}$ at the Tevatron) can be formulated as,

$$d\sigma(p\bar{p} \rightarrow c\bar{c}p) = \int dx_1 d\hat{\sigma}(gp \rightarrow c\bar{c}p) g(x_1, Q^2), \quad (1)$$

where x_1 is the longitudinal momentum fraction of the antiproton carried by the incident gluon. $g(x_1, Q^2)$ is the gluon density in the antiproton, and Q^2 is the scale of the hard process. $d\hat{\sigma}(gp \rightarrow c\bar{c}p)$ is the cross section for the partonic process $gp \rightarrow c\bar{c}p$.

In this section, we first give the formula for the partonic process $gp \rightarrow c\bar{c}p$ in the LLA QCD. In the leading order of perturbative QCD, there are nine diagrams shown in Fig.2, contributing to the partonic process $gp \rightarrow c\bar{c}p$. The two-gluon system coupled to the proton (antiproton) in Fig.2 is in a color-singlet state, which characterizes the diffractive processes in perturbative QCD. The two-gluon exchange model itself may not account for the full structure of the Pomeron, but it can approximate the description of diffractive processes in terms of perturbative QCD. Due to the positive signature of these diagrams (color-singlet exchange), we know that the real part of the amplitude cancels out in the leading logarithmic approximation. To evaluate the imaginary part of the amplitude, we must calculate the discontinuity represented by the crosses in each diagram of Fig.2.

The first four diagrams of Fig.2 are the same as those calculated in the diffractive photo-production processes. But, due to the existence of gluon-gluon interaction vertex in QCD, in the partonic process $gp \rightarrow c\bar{c}p$, there are additional five diagrams (Fig.2(5)-(9)). These five diagrams are needed for complete calculations in this order of QCD. From the following calculations, we can see that these five diagrams are important to cancel out the anomalous singularity which rises from the first four diagrams to obtain the correct results.

To calculate the imaginary part of the amplitude $\mathcal{A}(gp \rightarrow c\bar{c}+p)$, we employ the Feynman rule method [15]. For a cross check, we also use this method to calculate the diffractive charm jet photoproduction process $\gamma p \rightarrow c\bar{c}p$. In the leading logarithmic approximation, we can reproduce the results obtained previously by using the light-cone wave function method [4].

A. Kinematics and Sudakov variables

In the diffractive process $gp \rightarrow c\bar{c}p$, the final state only contains the charm quark and anti-charm quark. We set \vec{k}_T to be the transverse momentum of the charm quark, m_c the charm quark mass, and we define $m_T^2 = m_c^2 + k_T^2$. The invariant mass of the $c\bar{c}$ pair of the diffractive system is set to be M_X^2 , and x_{IP} is,

$$x_{IP} = \frac{M_X^2}{s}, \quad (2)$$

where s is the total c.m. energy of the gluon-proton system.

In our calculations, we express the formulas in terms of the Sudakov variables. That is, every four-momenta k_i are decomposed as,

$$k_i = \alpha_i q + \beta_i p + \vec{k}_{iT}, \quad (3)$$

where q and p are the momenta of the incident gluon and the proton, $q^2 = 0$, $p^2 = 0$, and $2p \cdot q = W^2 = s$. α_i and β_i are the momentum fractions of q and p respectively. k_{iT} is the transverse momentum, which satisfies

$$k_{iT} \cdot q = 0, \quad k_{iT} \cdot p = 0. \quad (4)$$

All of the Sudakov variables for every momentum are determined by using the on-shell conditions of the momenta of the external particles and the crossed lines in the diagram.

In the following, we calculate the differential cross section $d\hat{\sigma}/dt$ at $t = 0$. Namely, we set the momentum transfer squared of the diffractive process $gp \rightarrow c\bar{c}p$ equal to zero, i.e.,

$u^2 = t = 0$. $(q + u)$ is the momentum of the diffractive final state (contains charm and anticharm jets), and then

$$(q + u)^2 = M_X^2. \quad (5)$$

With this equation, and the on-shell conditions of the external proton lines,

$$(p - u)^2 = p^2 = 0, \quad (6)$$

we can determine the Sudakov variables associated with u as

$$\alpha_u = 0, \quad \beta_u = \frac{M_X^2}{s}, \quad \bar{u}_T^2 = 0. \quad (7)$$

In the diffractive region at hadron collisions, we know that $M_X^2 \ll s$, i.e., $\beta_u \ll 1$. So, in the following calculations, we set β_u to be a small parameter, and take the leading order contributions, and neglect the terms proportional to $\beta_u = \frac{M_X^2}{s}$.

α_k and β_k are determined from the on-shell conditions of the out-going charm quark and anticharm quark,

$$\begin{aligned} (k + q)^2 &= m_c^2, \\ (u - k)^2 &= m_c^2. \end{aligned} \quad (8)$$

By solving the above equations, we can obtain,

$$\begin{aligned} \alpha_k(1 + \alpha_k) &= -\frac{m_T^2}{M_X^2}, \\ \beta_k = -\alpha_k\beta_u &= -\frac{M_X^2}{s}\alpha_k. \end{aligned} \quad (9)$$

Because α_k is of order of 1, the value of m_T^2 is the same order as M_X^2 . From the last equation, we can see that β_k is much smaller than α_k , i.e., $|\beta_k| \ll |\alpha_k|$, because $\beta_u \ll 1$.

For the loop momentum l , we know that the integral of the amplitude over l_T receives large logarithmic contribution from the region $1/R_N^2 \ll l_T^2 \ll M_X^2$ (R_N is the nucleon radius) [2]. That is to say, the dominant contribution of the integration of l_T comes from the region $l_T^2 \ll M_X^2$, so l_T^2 is a small parameter compared with M_X^2 and m_T^2 . To calculate the integration of the amplitude over l_T^2 , we can expand the amplitude in terms of l_T^2 and take the leading order contributions.

The Sudakov variable α_l can be determined from the on-shell condition of the bottom cross on the proton line in each diagram of Fig.2, i.e.,

$$(p - l - u)^2 = 0, \quad (10)$$

which results in

$$\alpha_l = -\frac{l_T^2}{s}. \quad (11)$$

β_l is determined from the on-shell condition of the up cross on the charm quark line or the gluon line in each diagram. Unlike other variables calculated above the value of β_l

is not the same for these nine diagrams of Fig.2, because there are three different on-shell conditions of the up crossed lines,

$$(k - l - u)^2 = m_c^2, \quad \text{for Diag.1, 3, 5}, \quad (12)$$

$$(k + q + l)^2 = m_c^2, \quad \text{for Diag.2, 4, 6}, \quad (13)$$

$$(q + l + u)^2 = 0, \quad \text{for Diag.7, 8, 9}. \quad (14)$$

These three different relations lead to three different values for β_l ,

$$\beta_l = \frac{2(k_T, l_T) - l_T^2}{\alpha_k s}, \quad \text{for Diag.1, 3, 5}, \quad (15)$$

$$\beta_l = \frac{2(k_T, l_T) + l_T^2}{(1 + \alpha_k)s}, \quad \text{for Diag.2, 4, 6}, \quad (16)$$

$$\beta_l = -\frac{M_X^2 - l_T^2}{s}, \quad \text{for Diag.7, 8, 9}. \quad (17)$$

To obtain the above results, we have used the approximations: $\beta_u \ll 1$, and $|\beta_k| \ll |\alpha_k|$.

To end up the analysis of this subsection, we must note that there are two small parameters in the above calculations of the Sudakov variables,

$$\beta_u \ll 1, \quad \frac{l_T^2}{m_T^2} \ll 1. \quad (18)$$

And these two small parameters are the basic expansion parameters in the following calculations of the amplitude for the partonic process $gp \rightarrow c\bar{c}p$.

B. Expand the amplitude in terms of l_T^2

Using the variables induced in the above, we evaluate the differential cross section formula for the partonic process $gp \rightarrow c\bar{c}p$ as,

$$\frac{d\hat{\sigma}(gp \rightarrow c\bar{c}p)}{dt}|_{t=0} = \frac{dM_X^2 d^2 k_T d\alpha_k}{16\pi s^2 16\pi^3 M_X^2} \delta(\alpha_k(1 + \alpha_k) + \frac{m_T^2}{M_X^2}) \sum |\mathcal{A}|^2, \quad (19)$$

where \mathcal{A} is the amplitude of the process $gp \rightarrow c\bar{c}p$. We know that the real part of the amplitude \mathcal{A} is zero, and the imaginary part of the amplitude $\mathcal{A}(gp \rightarrow c\bar{c}p)$ for each diagram of Fig.2 has the following general form,

$$\text{Im}\mathcal{A} = C_F(T_{ij}^a) \int \frac{d^2 l_T}{(l_T^2)^2} F \times \bar{u}_i(k + q) \Gamma_\mu v_j(u - k), \quad (20)$$

where C_F is the color factor for each diagram, and a is the color index of the incident gluon. Γ_μ is some γ matrices including one propagator. F in the integral represents some other factor which is the same for each diagram,

$$F = \frac{3}{2s} g_s^3 f(x', x''; l_T^2), \quad (21)$$

where

$$f(x', x''; l_T^2) = \frac{\partial G(x', x''; l_T^2)}{\partial \ln l_T^2}, \quad (22)$$

where the function $G(x', x''; k_T^2)$ is the so-called off-diagonal gluon distribution function [5]. Here, x' and x'' are the momentum fractions of the proton carried by the two gluons. It is expected that for small x , there is no large difference between the off-diagonal and the usual diagonal gluon densities [16]. So, in the following calculations, we estimate the production rate by approximating the off-diagonal gluon density by the usual diagonal gluon density, $G(x', x''; Q^2) \approx xg(x, Q^2)$, where $x = x_{IP} = M_X^2/s$. Later we will discuss the off-diagonal parton distribution function effects for the diffractive charm jet production process calculated here and J/ψ production.

The color factors C_F are not the same for the nine diagrams, and they are

$$\begin{aligned} C_F &= \frac{2}{9}, & \text{for Diag.1, 4,} \\ C_F &= -\frac{1}{36}, & \text{for Diag.2, 3,} \\ C_F &= \frac{1}{4}, & \text{for Diag.5, 8,} \\ C_F &= -\frac{1}{4}, & \text{for Diag.6, 9,} \\ C_F &= -\frac{1}{2}, & \text{for Diag.7,} \end{aligned} \quad (23)$$

respectively.

As mentioned above, to calculate the leading logarithmic results for the partonic process $gp \rightarrow c\bar{c}p$, the amplitude of each diagram must be expanded in terms of l_T^2 . From the integral of Eq. (20), we can see that the large logarithmic contribution comes from the region $l_T^2 \ll M_X^2$. So, the leading logarithmic contribution to the cross section of the partonic process comes from the terms in Γ_μ which are proportional to l_T^2 . Because we are interested in the leading logarithmic results of the cross section, we neglect the higher order terms of l_T^2 in Γ_μ .

Furthermore, in the integral of Eq. (20) the l_T^0 terms in Γ_μ coming from all diagrams must be canceled out by each other. Otherwise, their net sum (order of l_T^0) will lead to a linear singularity when we perform the integration over l_T^2 . The linear singularity is not proper in QCD calculations. So, we first observe the amplitude behavior at the order of l_T^0 , i.e., in the limit of $l_T^2 \rightarrow 0$. In this limit, the Γ_μ for each diagram has the following result,

$$\begin{aligned} \Gamma_\mu^{(1)} &= -\Gamma_\mu^{(3)} = -\Gamma_\mu^{(5)} = \frac{s^2}{M_X^2} \alpha_k \gamma_\mu, \\ \Gamma_\mu^{(2)} &= -\Gamma_\mu^{(4)} = -\Gamma_\mu^{(6)} = \frac{s^2}{M_X^2} (1 + \alpha_k) \gamma_\mu, \\ \Gamma_\mu^{(7)} &= \Gamma_\mu^{(8)} = -\Gamma_\mu^{(9)} = -\frac{s^2}{M_X^2} \gamma_\mu - \not{p}_\mu p_\mu. \end{aligned} \quad (24)$$

The second terms in $\Gamma_\mu^{(7)}$, $\Gamma_\mu^{(8)}$ and $\Gamma_\mu^{(9)}$ come from the contributions of β_l terms. This is because $\beta_l = -\frac{M_X^2}{s} \neq 0$ in the limit $l_T^2 \rightarrow 0$. To obtain the above results, we have used the following identities,

$$\begin{aligned} \bar{u}(k+q)(\not{k} + \not{q} - m_c) &= 0, \\ (\not{u} - \not{k} + m_c)v(u-k) &= 0, \\ \bar{u}(k+q)(\not{q} + \not{u})v(u-k) &= \bar{u}[(\not{k} + \not{q} - m_c) + (\not{u} - \not{k} + m_c)]v = 0. \end{aligned} \quad (25)$$

With the values of the color factor C_F for the diagrams given in Eq. (23), we find that their sum is zero. That is to say, there is no contribution to the amplitude of the partonic process $gp \rightarrow c\bar{c}p$ in this order (Γ_μ takes the order of l_T^0). As mentioned above, this is what we expected. If there are only the first four diagrams (the same as those in photoproduction processes), their contributions of the order of l_T^0 can not be canceled out by each other, because their color factors are not the same for Diag.1,4 and Diag.2,3. (In photoproduction processes, the color factors for these four diagrams are the same, so their contribution is zero at the order of l_T^0 .) However, as mentioned above, QCD gauge invariance requires the appearance of other five diagrams at the same order of coupling constant of strong interaction. The contributions from Diag.5 and 6 cancel out the linear singularity which rises from the first four diagrams. The linear singularity from the last three diagrams, Diag.7, 8, and 9, are canceled out by each other. So, the amplitude has no linear singularity now.

From the above analysis, we see that the first four diagrams alone cannot give a gauge invariant part of the amplitude for the partonic process $gp \rightarrow c\bar{c}p$.

At the next order expansions of Γ_μ , l_T^2 , the evaluation is much more complicated. We first give the expansion results for the propagators in Γ_μ for every diagrams. To the order of l_T^2 , the expansions of these propagators are,

$$\begin{aligned} g_1 &= \frac{1}{\alpha_k M_X^2}, \quad g_4 = -\frac{1}{(1 + \alpha_k) M_X^2}, \\ g_2 &= \frac{1}{\alpha_k M_X^2} \left[1 - \frac{2(k_T, l_T)}{m_T^2} - \frac{l_T^2}{m_T^2} + \frac{4(k_T, l_T)^2}{(m_T^2)^2} \right], \\ g_3 &= -\frac{1}{(1 + \alpha_k) M_X^2} \left[1 + \frac{2(k_T, l_T)}{m_T^2} - \frac{l_T^2}{m_T^2} + \frac{4(k_T, l_T)^2}{(m_T^2)^2} \right], \\ g_5 &= \frac{1}{M_X^2} \left[1 - \frac{2(k_T, l_T)}{\alpha_k M_X^2} + \frac{(1 + \alpha_k) l_T^2}{\alpha_k M_X^2} + \frac{4(k_T, l_T)^2}{(\alpha_k M_X^2)^2} \right], \\ g_6 &= \frac{1}{M_X^2} \left[1 - \frac{2(k_T, l_T)}{(1 + \alpha_k) M_X^2} + \frac{\alpha_k l_T^2}{(1 + \alpha_k) M_X^2} + \frac{4(k_T, l_T)^2}{((1 + \alpha_k) M_X^2)^2} \right], \\ g_7 &= \frac{1}{M_X^2}, \quad g_8 = \frac{1}{\alpha_k} g_5, \quad g_9 = -\frac{1}{1 + \alpha_k} g_6. \end{aligned} \quad (26)$$

Apart from the propagator expansions, the γ matrices in Γ_μ also contain the l_T^2 terms. They are mostly coming from the Sudakov variables (expressed in l_T^2) of momentum l , i.e., $\alpha_l = \frac{l_T^2}{s}$, β_l , and the slasher \not{l}_T . Furthermore, the 2-dimensional product (k_T, l_T) also contributes l_T^2 terms. After integrating the azimuth angle of \not{l}_T , we will get the following results,

$$\begin{aligned} \int d^2 l_T (k_T, l_T)^2 &= \frac{\pi}{2} \int d l_T^2 k_T^2 l_T^2, \\ \int d^2 l_T (k_T, l_T) \not{l}_T &= \frac{\pi}{2} \int d l_T^2 \not{k}_T l_T^2. \end{aligned} \quad (27)$$

To test the validity of our procedure, we first evaluate the expansions of Γ_μ for the first four diagrams, and use these expansions to calculate the amplitude for the diffractive photoproduction processes $\gamma p \rightarrow c\bar{c}p$. To do this, we only need do the following changes in the amplitude formula Eq. (20),

$$C_F T_{ij}^a \rightarrow \frac{2}{9} \delta_{ij}. \quad (28)$$

To the order of l_T^2 , the expansions of Γ_μ for the first four diagrams are:

$$\begin{aligned} \Gamma_\mu^{(1)} &= \Gamma_\mu^{(4)} = \frac{l_T^2}{M_X^2} s \gamma_\mu, \\ \Gamma_\mu^{(2)} &= \frac{l_T^2}{M_X^2} \left[-\not{p} \not{q} \gamma_\mu - \frac{1 + \alpha_k}{\alpha_k} \gamma_\mu \not{q} \not{p} + \frac{1}{\alpha_k} \not{p} \gamma_\mu \not{p} + \frac{k_T^2 - m_c^2}{(m_T^2)^2} s^2 (1 + \alpha_k) \gamma_\mu \right. \\ &\quad \left. - \frac{1}{\alpha_k m_T^2} (\alpha_k s \not{p} \not{k}_T \gamma_\mu + (1 + \alpha_k) s \gamma_\mu \not{k}_T \not{p}) \right], \\ \Gamma_\mu^{(3)} &= \frac{l_T^2}{M_X^2} \left[-\gamma_\mu \not{q} \not{p} - \frac{\alpha_k}{1 + \alpha_k} \not{p} \not{q} \gamma_\mu - \frac{1}{1 + \alpha_k} \not{p} \gamma_\mu \not{p} - \frac{k_T^2 - m_c^2}{(m_T^2)^2} s^2 \alpha_k \gamma_\mu \right. \\ &\quad \left. + \frac{1}{(1 + \alpha_k) m_T^2} (\alpha_k s \not{p} \not{k}_T \gamma_\mu + (1 + \alpha_k) s \gamma_\mu \not{k}_T \not{p}) \right]. \end{aligned} \quad (29)$$

Using these expansions, together with Eqs. (28), (19) and (20), we obtain the cross section formula for the diffractive photoproduction process $\gamma p \rightarrow c\bar{c}p$, which is consistent with the LLA result calculated via light-cone wave function approach (for $Q^2 = 0$) [4].

For the last five diagrams, the expansions of Γ_μ are more complicated. To simplify our calculations, the contributions of these five diagrams including the color factor C_F are added together, and decomposed into several terms as follows.

The terms (defined as a -term) coming from the slasher \not{l}_T in the γ matrices, for all these five diagrams to sum up together, are

$$C_F \Gamma_\mu^{(a)} = -\frac{l_T^2}{M_X^2} \left(1 + \frac{1}{4\alpha_k(1 + \alpha_k)} \right) \not{p} p_\mu. \quad (30)$$

The terms (b -term) from $\alpha_l = -\frac{l_T^2}{M_X^2}$ are

$$C_F \Gamma_\mu^{(b)} = \frac{l_T^2}{4M_X^2} \left[\left(4 + \frac{1}{\alpha_k(1 + \alpha_k)} \right) \beta_u \not{p} p_\mu - \frac{1 + \alpha_k}{\alpha_k} \gamma_\mu \not{q} \not{p} - \frac{\alpha_k}{1 + \alpha_k} \not{p} \not{q} \gamma_\mu - \frac{3}{2} s \gamma_\mu \right]. \quad (31)$$

The terms (c -term) from β_l are

$$C_F \Gamma_\mu^{(c)} = \frac{l_T^2}{2M_X^2} \not{p} p_\mu \left[\frac{k_T^2}{m_T^2} - \frac{1}{2} \left(1 - \frac{2k_T^2}{m_T^2} \right) \frac{\alpha_k^2 + (1 + \alpha_k)^2}{\alpha_k(1 + \alpha_k)} \right]. \quad (32)$$

The terms (d -term) from propagator expansions are

$$C_F \Gamma_\mu^{(d)} = \frac{l_T^2}{4(M_X^2)^2} s^2 \gamma_\mu \left[\frac{\alpha_k^3 - (1 + \alpha_k)^3}{\alpha_k(1 + \alpha_k)} + \frac{2k_T^2}{M_X^2} \frac{\alpha_k^3 - (1 + \alpha_k)^3}{\alpha_k^2(1 + \alpha_k)^2} \right]. \quad (33)$$

The last term comes from such terms which are proportional to “ (k_T, l_T) \not{k}_T ”. They are (e -term)

$$C_F \Gamma_\mu^{(e)} = \frac{l_T^2}{4(M_X^2)^2} \left[-\frac{1 + \alpha_k}{\alpha_k} (2\alpha_k s \not{p} k_T^\mu + s \gamma_\mu \not{k}_T \not{p} - \not{q} \not{k}_T \not{p} p_\mu - \alpha_k s \not{k}_T p_\mu) \right. \\ \left. + \frac{\alpha_k}{1 + \alpha_k} (2(1 + \alpha_k) s \not{p} k_T^\mu - s \not{p} \not{k}_T \gamma_\mu + \not{p} \not{k}_T \not{q} p_\mu - (1 + \alpha_k) s \not{k}_T p_\mu) \right]. \quad (34)$$

Adding up all of the above a, b, c, d, e terms, and those terms coming from the first four diagrams in Eq. (29), we get the amplitude squared for the diffractive process $gp \rightarrow c\bar{c}p$ as, averaged over the spin and color freedoms,

$$\sum |\overline{\mathcal{A}}|^2 = \frac{\alpha_s^3 \pi^5}{9(M_X^2)^4 (m_T^2)^4} m_c^2 s^2 (m_T^2 M_X^2 - 8k_T^2 m_c^2) (10M_X^2 - 27m_T^2)^2 (xg(x, Q^2))^2, \quad (35)$$

where the scale Q^2 is set to be $Q^2 = m_T^2$. The factorization scale in the gluon density is very important because we know that the parton distributions at small x change rapidly with this scale. Here, we choose the scale to be m_T^2 which is typically used in the calculations of the heavy quark production processes. In Ref. [14], they used different scales for their two parts of their diagrams for the partonic process. However, as discussed in the above calculations, all of the nine diagrams must be summed together to give a gauge invariant amplitude for the coherent diffractive charm jet production at hadron colliders. So, the scales of the nine diagrams must be the same. The separation in [14] is not gauge invariant.

Finally, the cross section for the partonic process $gp \rightarrow c\bar{c} + p$, in the LLA of perturbative QCD, is

$$\frac{d\hat{\sigma}(gp \rightarrow c\bar{c} + p)}{dt} \Big|_{t=0} = \frac{dM_X^2 dk_T^2}{(M_X^2 m_T^2)^4} \frac{\pi^2 \alpha_s^3}{128 \times 9} \frac{m_c^2}{\sqrt{M_X^2 (M_X^2 - 4m_T^2)}} \\ (M_X^2 m_T^2 - 8k_T^2 m_c^2) (10M_X^2 - 27m_T^2)^2 (xg(x, Q^2))^2. \quad (36)$$

The integral region of k_T^2 satisfies the following constrain

$$k_T^2 \leq \frac{M_X^2}{4} - m_c^2. \quad (37)$$

From Eq.(36), we can see that the cross section of diffractive light quark (high k_T) jet hadroproduction vanishes as m_q^2 (m_q is the quark mass) in the leading logarithmic approximation of perturbative QCD (see also [17]).

III. NUMERICAL RESULTS

With the cross section formula Eq. (36) for the partonic process $gp \rightarrow c\bar{c}p$, we can get the cross section of diffractive production at the hadron level. However, as mentioned

above, there exist nonfactorization effects caused by the spectator interactions in the hard diffractive processes in hadron collisions. Here, we use a suppression factor \mathcal{F}_S to describe this nonfactorization effects in the hard diffractive processes at hadron colliders [10]. At the Tevatron, the value of \mathcal{F}_S may be as small as $\mathcal{F}_S \approx 0.1$ [10,11]. That is to say, the total cross section of the diffractive processes at the Tevatron may be reduced down by an order of magnitude due to the nonfactorization effects. In the following numerical calculations, we adopt this suppression factor value to evaluate the diffractive production rate of charm jet at the Fermilab Tevatron.

Our numerical results are plotted in Fig.3 to Fig.7. From Eq. (36), we can see that the cross section is sensitive to the gluon density in the proton. In fact, the cross section for $p\bar{p} \rightarrow c\bar{c}p$ behaves as

$$d\sigma \propto g(x_1, Q^2)(g(x, Q^2))^2, \quad (38)$$

where x_1 is the longitudinal momentum fraction of the proton (or antiproton) carried by the incident gluon. So, the c.m. energy of the gluon-proton system is $s = x_1 S$, where S is the total c.m. energy of the proton and proton (antiproton) system (e.g., $S = (1800\text{GeV})^2$ at the Tevatron). Then, $x = x_{IP} = M_X^2/s = M_X^2/x_1 S$. We can see that at the Tevatron, x may be lowered down to the $10^{-6} \sim 10^{-5}$ level (varying with the lower bound of the transverse momentum k_T for the observation).

In the high energy diffractive processes, we know that the relation $M_X^2 \ll s = x_1 S$ must be satisfied (in our calculations, we set $M_X^2/s < 0.1$). Together with Eq. (37), these constrains will give the integration bound of the arguments x_1 , M_X^2 , and k_T^2 .

In our calculations, the charm quark mass is set to be $m_c = 1.5\text{GeV}$, and the scale of the running coupling constant of strong interaction is set to be $Q^2 = m_T^2$. For the gluon distribution function, we choose the GRV NLO set [18].

In Fig.3, we show the M_X^2 dependence of the differential cross section $d^2\sigma/dtdM_X^2|_{t=0}$ for the diffractive charm jet production at the Tevatron. In Fig.4, we plot the cross section $d\sigma/dt|_{t=0}$ as a function of lower bound of the transverse momentum k_T . From this figure, we can see that the cross section is sensitive to the lower bound of k_T . It decreases rapidly as $k_{T\min}$ increases. In this figure, we also plot the cross section for bottom quark jet diffractive production by using the same formula Eq. (36) except changing the quark mass from $m_c = 1.5\text{ GeV}$ to $m_b = 4.9\text{ GeV}$. The difference of these two curves shows the dependence of the cross section on the quark mass. From Eq. (36), we can see that at large k_T ($k_T \gg m_b$), the cross section is proportional to the quark mass, so the cross section of bottom jet is larger than that of charm jet. However, due to the existence of the power factor of $1/m_T^2 = 1/(k_T^2 + m_q^2)$ in the cross section formula, at small k_T smaller quark mass will result in larger cross section. So, the cross section of charm jet is larger than that of bottom jet at small $k_{T\min}$.

In Fig.5-7, we show the sensitivity of the cross section to the gluon distribution in the proton. In Fig.5, we select $x_{1\min}$ as argument to show the behavior of the differential cross section $d\sigma/dt|_{t=0}$ as a function of $x_{1\min}$. We can see that most contribution comes from $x_1 > 10^{-2}$ region. In Fig.6, we plot the cross section as a function of x_{\max} , which shows that most contribution comes from $x \sim 10^{-3} - 10^{-2}$ region. In these two figures, for both we set the lower cut of the transverse momentum k_T to be $k_{T\min} = 5\text{ GeV}$. From Fig.4, we see that the lower bound of transverse momentum $k_{T\min}$ largely affects the total cross section of this

process. Furthermore, it is expected that $k_{T\min}$ can also affect the relative importance of different x region contribution to the total cross section. This effect can be seen from Fig.7. In this figure, we plot the ratio σ/σ_{tot} as a function of x_{\max} , where σ_{tot} is the total cross section after integrating over all x region, while σ is the cross section with the upper bound x_{\max} for x . From left to right, these three curves correspond to three different lower bound of transverse momentum, $k_{T\min} = 0, 5, 10 \text{ GeV}$ respectively. From Fig.7, we see that for smaller value of $k_{T\min}$, the dominant contribution comes from smaller x region.

As stated in the section of Introduction, the nine diagrams in our calculations all contribute to the coherent diffractive charm jet production at hadron colliders. So, the above calculated numerical results from Figs.3-7 are all for the coherent diffractive production.

IV. THE OFF-DIAGONAL GLUON DISTRIBUTION EFFECTS

The off-diagonal parton distribution function is a hot topic in recent years [19]. Typically, the off-diagonal distribution has two different regions. One is $x' > x_{IP}$ ($x'' > 0$, because $x' - x'' = x_{IP}$), and the other is $x' < x_{IP}$. For the off-diagonal gluon distribution function $G(x', x''; Q^2)$, x' and x'' are the momentum fractions of the proton carried by the outgoing gluon and the returning gluon respectively. In the first region, because $x'' > 0$, $G(x', x''; Q^2)$ is similar to the usual gluon distribution function $g(x; Q^2)$. However, in the second region ($x'' < 0$), $G(x', x''; Q^2)$ is rather a distribution amplitude of taking two gluons out of the proton, which is similar to a meson's wave function. Previous studies [16] have shown that in the first region, the off-diagonal gluon distribution function is not very different from the usual diagonal gluon distribution at small x . So, in this region we can safely approximate the off-diagonal gluon distribution function by the diagonal distribution. On the other hand, in the region of $x' < x_{IP}$, where the off-diagonal gluon distribution function is distinctively different from the traditional diagonal gluon distribution function [20], the off-diagonal distribution function effects may be important.

From Fig.2, we find that there are three different values for x' (x'') because there are three different values for β_l ,

$$\begin{aligned} x' = \beta_l + \beta_u &= x_{IP} + \frac{2(k_T, l_T) - l_T^2}{\alpha_k s} \quad \text{for Diag.1, 3, 5,} \\ &= x_{IP} + \frac{2(k_T, l_T) + l_T^2}{(1 + \alpha_k)s} \quad \text{for Diag.2, 4, 6,} \\ &= \frac{l_T^2}{s} \quad \text{for Diag.7, 8, 9.} \end{aligned} \quad (39)$$

When integrating the amplitude over \vec{l}_T , x' may be smaller than x_{IP} in some region, where the off-diagonal gluon distribution function $G(x', x''; l_T^2)$ will take its value in the second region. Especially, for Diag.7-9, the dominant contribution to the integration of the amplitude comes from the region where x' is mostly smaller than x_{IP} , because the large logarithm contribution of the integration comes from the region of $x' \ll x_{IP}$ ($l_T^2 \ll M_X^2$). So, we can expect that the off-diagonal effects on this process may be important.

In our previous calculations of the diffractive J/ψ production at hadron colliders, we also neglect the off-diagonal gluon distribution function effects. However, from Fig.2 of Ref. [6], we see that x' has two different values,

$$\begin{aligned}
x' &= \frac{M_X^2 + 2l_T^2}{s} = x_{IP} + \frac{2l_T^2}{s}, \quad \text{for Diag. } a, b, c, \\
&= \frac{l_T^2}{s}, \quad \text{for Diag. } d, e.
\end{aligned} \tag{40}$$

When integrating the amplitude over l_T^2 , the off-diagonal gluon distribution functions for Diag.*a*, *b*, *c* take their values in the region of $x' < x_{IP}$, in which we can safely use the usual gluon distribution instead. However, for Diag.*d*, *e*, the off-diagonal gluon distributions dominantly take their values in the region of $x' < x_{IP}$ (because the large logarithmic contribution to the amplitude comes from the integral region $l_T^2 \ll M_\psi^2$). So, the off-diagonal distribution effects in the diffractive J/ψ production at hadron colliders are also expected to be very important.

To evaluate the off-diagonal distribution effects on the diffractive processes (charm jet and J/ψ production at hadron colliders) discussed above, we must integrate the amplitude including the differential off-diagonal gluon distribution function $f(x', x''; l_T^2)$ in Eq. (22) (with the evolution scale at $Q^2 = l_T^2$) over l_T^2 numerically. This task is difficult and beyond the scope of this paper. Further investigation in this direction is in progress.

V. CONCLUSIONS

In this paper, we have calculated the diffractive charm jet production at hadron colliders in perturbative QCD by using the two-gluon exchange model. Differing significantly from other models, our coherent diffractive amplitude for the partonic process is gauge invariant and contains no linear singularities as $l_T^2 \rightarrow 0$. We give the formula for the cross section of this process in the leading logarithmic approximation. By neglecting the off-diagonal gluon distribution effects, we have estimated the production rate of diffractive charm jet production at the Tevatron. The comparison of production rates between the charm jet and the bottom jet has shown the dependence of the cross section on the quark mass, which is a distinctive feature of these processes. We have also discussed the off-diagonal gluon distribution effects on this process and the hard diffractive J/ψ production previously calculated [6].

In conclusion, we have calculated the heavy quark jet production in the diffractive processes, which belongs to the coherent diffractive processes at hadron colliders. Detecting the heavy quark jet in hadron collisions would provide strong signals for these coherent diffractive processes. We note that the process calculated in this paper is gluon initiated process, which is sensitive to small- x gluon distribution in the proton. Some other processes, such as W^\pm , Drell-Yan processes, are quark initiated processes, which would be sensitive to the large- x quark distribution function in the proton [9]. Work in this direction is in progress.

ACKNOWLEDGMENTS

This work was supported in part by the National Natural Science Foundation of China, the State Education Commission of China, and the State Commission of Science and Technology of China.

REFERENCES

- [1] P.D.B. Collins, *An introduction to Regge theory and high energy physics*, Cambridge University Press, Cambridge (1977).
- [2] M.G. Ryskin, Z. Phys. **C37**, 89 (1993); M.G. Ryskin, et al., Z. Phys. **C76**, 231 (1996).
- [3] S.J. Brodsky et al., Phys. Rev. **D50**, 3134 (1994); L. Frankfurt et al., Phys. Rev. **D57**, 512 (1998).
- [4] T. Gehrmann and W.J. Stitling, Z. Phys. **C70**, 69 (1996); M. Genovese et al., Phys. Lett. **B378**, 347 (1996); E.M. Levin et al., hep-ph/9606443.
- [5] X. Ji, Phys. Rev. Lett. **78**, 610 (1997), Phys. Rev. **D55**, 7114 (1997); A.V. Radyushkin, Phys. Lett. **B385**, 333 (1996), Phys. Lett. **B380**, 417 (1996), Phys. Rev. **D56**, 5524 (1997).
- [6] F. Yuan, J.S. Xu, H.A. Peng, and K.T. Chao, Phys. Rev. **D58**, 114016 (1998).
- [7] G. T. Bodwin, E. Braaten and G. P. Lepage, Phys. Rev. **D 51**, 1125 (1995).
- [8] P.V. Landshoff and J.C. Polkinghorne, Nucl. Phys. **B33**, 221 (1971), **B36**, 642 (1972); F. Henyey and R. Savit, Phys. Lett. **B52**, 71 (1974); J.L. Cardy and G.A. Winbow, Phys. Lett. **B52**, 95 (1974); C. DeTar, S.D. Ellis and P.V. Landshoff, Nucl. Phys. **B87**, 176 (1975).
- [9] J.C. Collins, L. Frankfurt and M. Strikman, Phys. Lett. **B307**, 161 (1993);
- [10] D.E. Soper, talk at DIS97 conference, Chicago, April 1997, hep-ph/9707384.
- [11] F. Abe et al., Phys. Rev. Lett. **78**, 2698 (1997); F. Abe et al., Phys. Rev. Lett. **79**, 2636 (1997).
- [12] J.D. Bjorken, Phys. Rev. **D45**, 4077 (1992); **D47**, 10 (1993); E. Gotsman, E. Levin and U. Maor, Phys. Lett. **B309**, 199 (1993); Nucl. Phys. **B493**, 354 (1997); hep-ph/9804404; R.S. Fletcher, Phys. Rev. **D48**, 5162 (1993). A.D. Martin, M.G. Ryskin and V.A. Khoze, Phys. Rev. **D56**, 5867 (1997).
- [13] G. Ingelman and P. Schlein, Phys. Lett. **B 152**, 256 (1985).
- [14] G. Alves, E. Levin, and A. Santoro, Phys. Rev. **D55**, 2683 (1997).
- [15] E. Levin and M. Wüsthoff, Phys. Rev. **D50**, 4306 (1994).
- [16] P. Hoodbhoy, Phys. Rev. **D56**, 388 (1997); L. Frankfurt et al., Phys. Lett. **B418**, 345 (1998); A.D. Martin and M.G. Ryskin, Phys. Rev. **D57**, 6692 (1998).
- [17] F. Yuan and Kuang-Ta Chao, hep-ph/9904237, for the publication version please see hep-ph/9907371, to appear in Phys. Rev. D.
- [18] M. Glück et al. Z. Phys. **C67**, 433 (1995).
- [19] For a recent review on this subject, see X. Ji, J. Phys. G. 24, 1181 (1998).
- [20] K. Golec-Biernat, J. Kwiecinski, and A.D. Martin, Preprint DTP/98/12.

Figure Captions

Fig.1. Sketch diagram for the diffractive charm jet production at hadron colliders in perturbative QCD.

Fig.2. The lowest order perturbative QCD diagrams for partonic process $gp \rightarrow c\bar{c}p$.

Fig.3. The differential cross section $d^2\sigma/dtdM_X^2|_{t=0}$ at the Fermilab Tevatron as a function of M_X^2 .

Fig.4. The differential cross section $d\sigma/dt|_{t=0}$ after integrating over k_T^2 (for $k_T^2 \geq k_{T\min}^2$) as a function of $k_{T\min}$, where $m_c = 1.5 \text{ GeV}$ for the charm jet and $m_b = 4.9 \text{ GeV}$ for the bottom jet.

Fig.5. The differential cross section $d\sigma/dt|_{t=0}$ as a function of $x_{1\min}$, where $x_{1\min}$ is the lower bound of x_1 in the integration of the cross section.

Fig.6. The differential cross section $d\sigma/dt|_{t=0}$ as a function of x_{\max} , where x_{\max} is the upper bound in the integration of the cross section.

Fig.7. The ration σ/σ_{tot} as a function of x_{\max} , where σ_{tot} is the total cross section after integrating over all x region. From left to right, the three curves correspond to three lower bounds of transverse momentum, $k_{T\min} = 0, 5, 10 \text{ GeV}$ respectively.

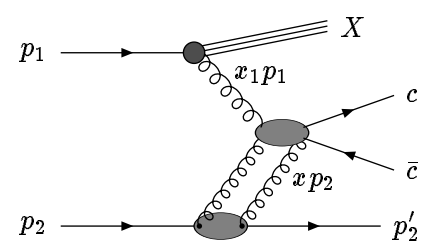


Fig.1

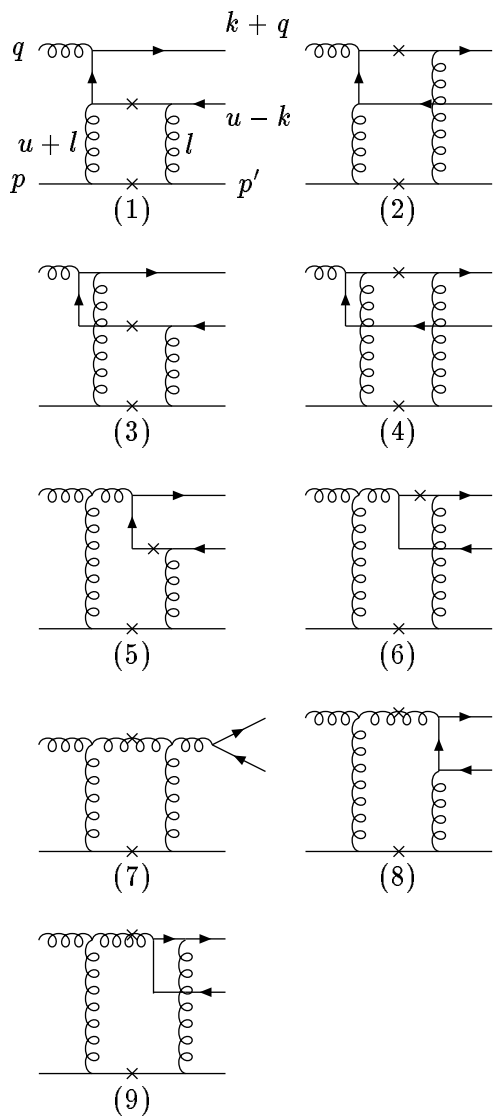


Fig.2

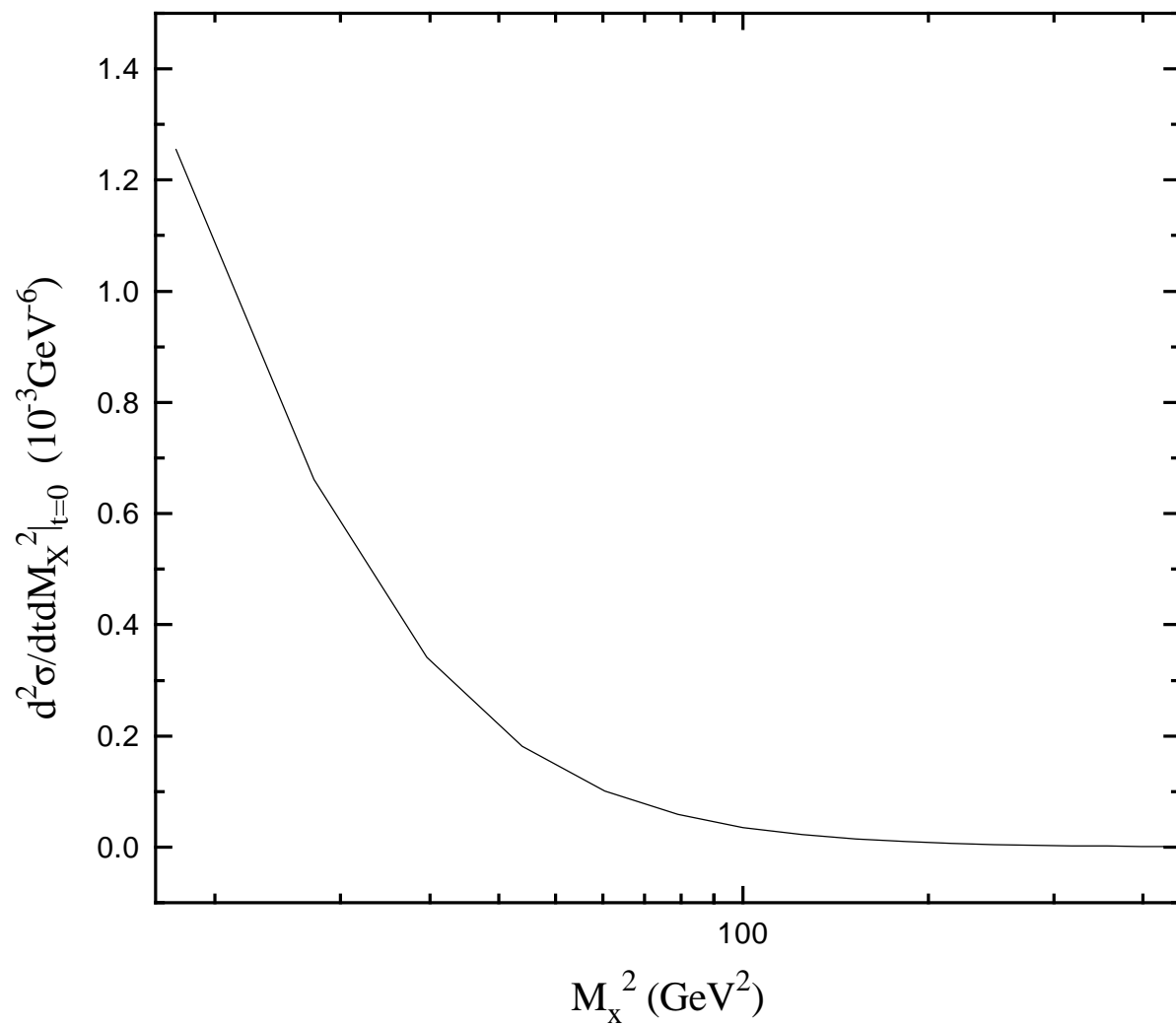


Fig.3

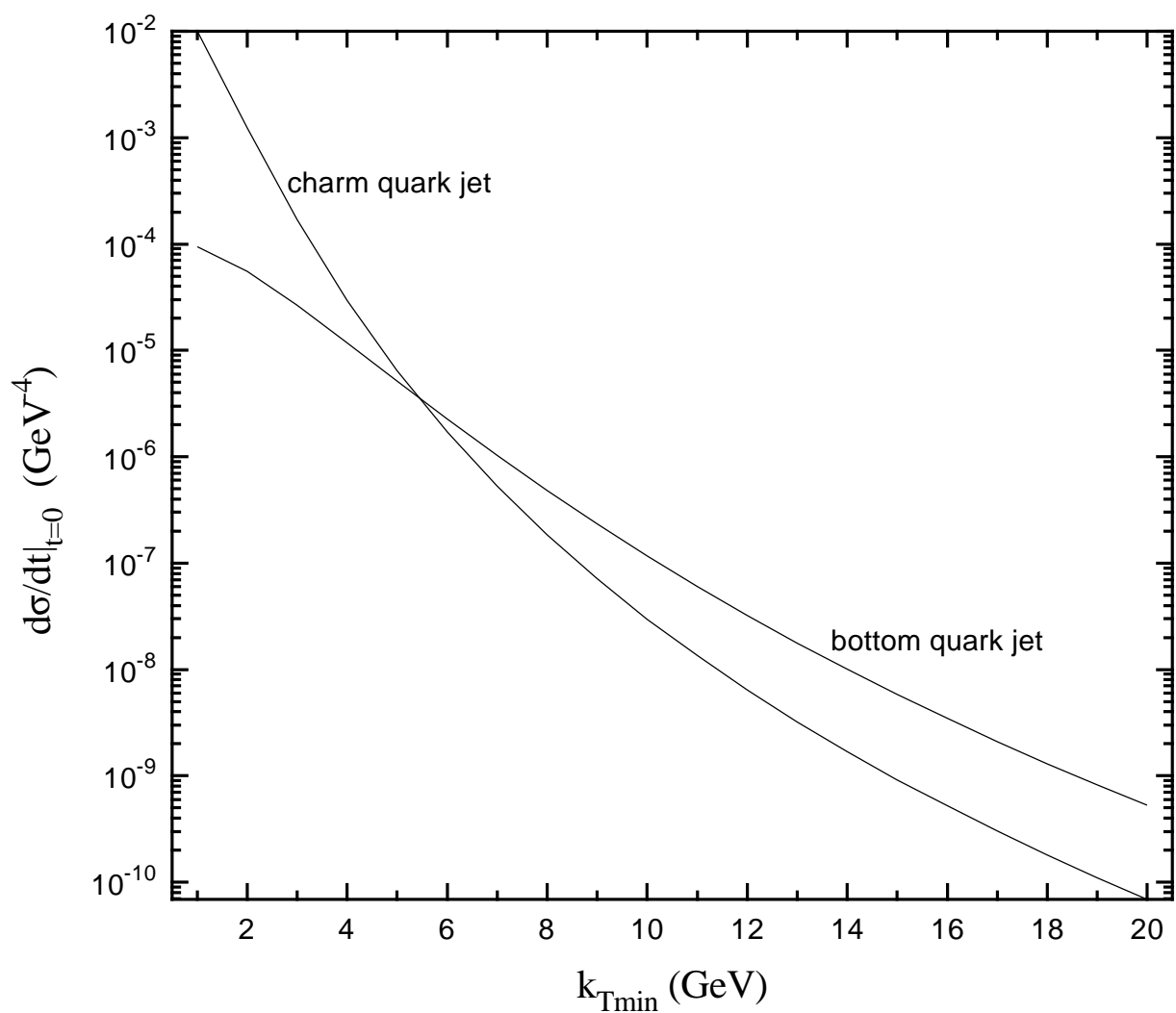


Fig.4

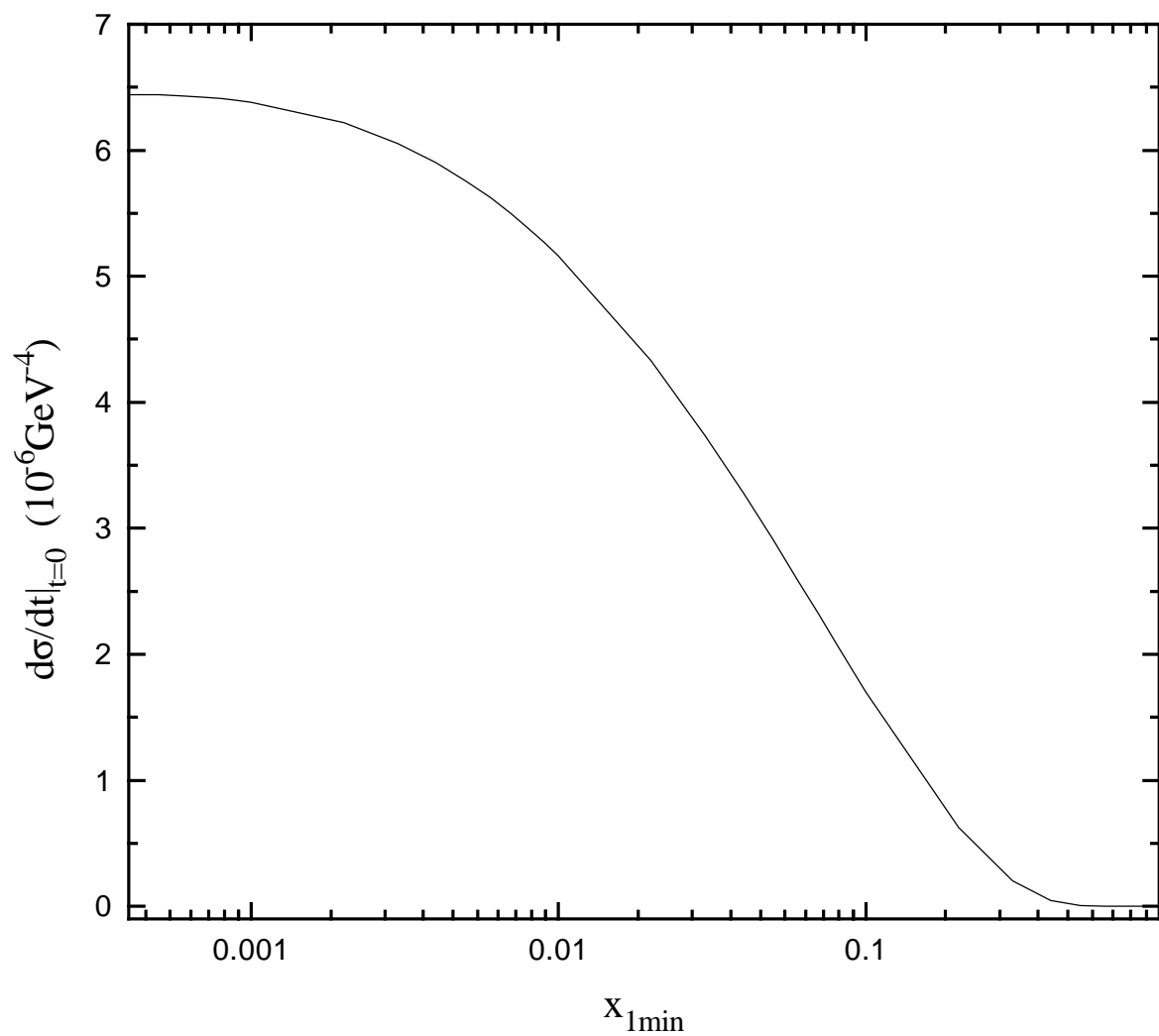


Fig.5

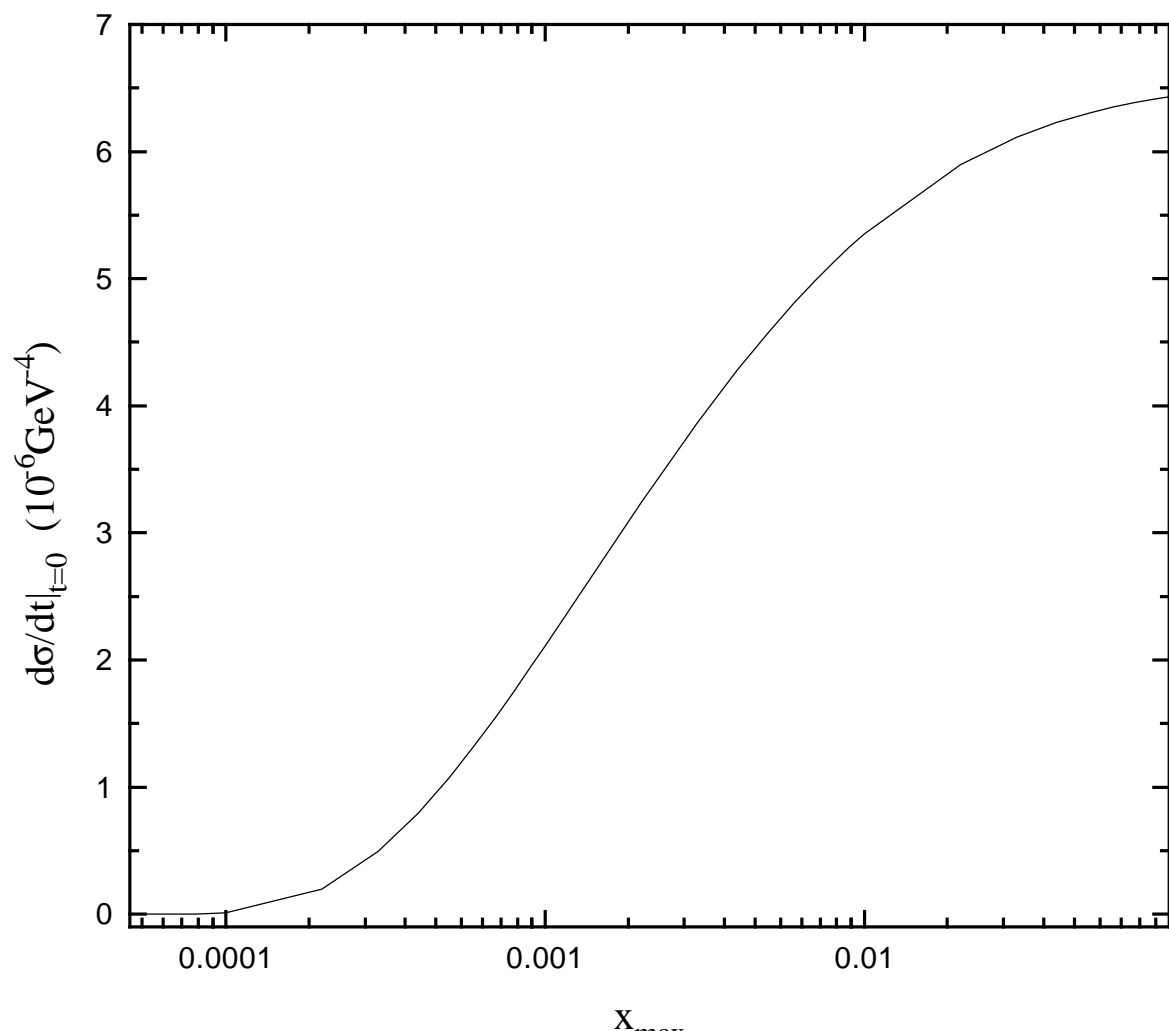


Fig.6

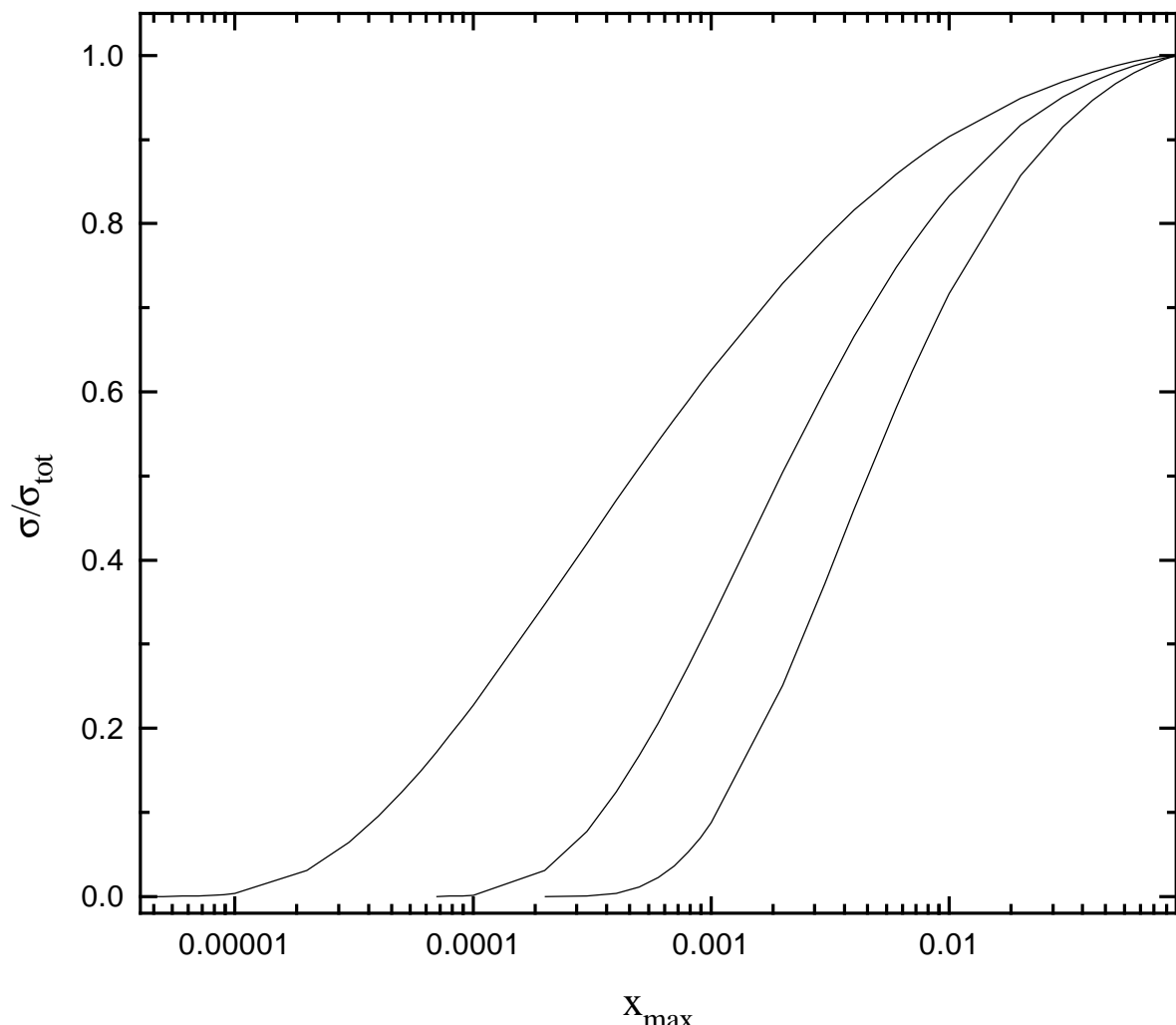


Fig.7